Hindawi
International Transactions on Electrical Energy Systems
Volume 2023, Article ID 6777135, 21 pages
https://doi.org/10.1155/2023/6777135

Research Article

Analysis of Pre- and during COVID-19 Mixed Load Models on Unbalanced Radial Distribution System Using a New Metaphor-Less Rao Optimization

Jitendra Singh Bhadoriya,[1] **A. R. Gupta**,[1,2] **and Baseem Khan**[3,4]

[1]*Department of Electrical Engineering, National Institute of Technology, Kurukshetra, Haryana, India*
[2]*Shri Phanishwar Nath Renu Engineering College Araria, DST Govt of Bihar, Araria, India*
[3]*Department of Electrical and Computer Engineering, Hawassa University, Hawassa 05, Ethiopia*
[4]*Department of Project Management, Universidad Internacional Iberoamericana, Campeche 24560, Mexico*

Correspondence should be addressed to Baseem Khan; basseemk@hu.edu.et

Received 10 June 2022; Revised 8 October 2022; Accepted 7 February 2023; Published 14 March 2023

Academic Editor: Ci Wei Gao

An unbalanced electrical distribution system (DS) with radial construction and passive nature suffers from significant power loss. The unstable load demand and poor voltage profile resulted from insufficient reactive power in the DS. This research implements a unique Rao algorithm without metaphors for the optimal allocation of multiple distributed generation (DG) and distribution static compensators (DSTATCOM). For the appropriate sizing and placement of the device, the active power loss, reactive power loss, minimum value of voltage, and voltage stability index are evaluated as a multiobjective optimization to assess the device's impact on the 25-bus unbalanced radial distribution system. Various load models, including residential, commercial, industrial, battery charging, and other dispersed loads, were integrated to develop a mixed load model for examining electrical distribution systems. The impact of unpredictable loading conditions resulting from the COVID-19 pandemic lockdown on DS is examined. The investigation studied the role of DG and DSTATCOM (DGDST) penetration in the electrical distribution system for variations in different load types and demand oscillations under the critical emergency conditions of COVID-19. The simulation results produced for the mixed load model during the COVID-19 scenario demonstrate the proposed method's efficacy with distinct cases of DG and DSTATCOM allocation by lowering power loss with an enhanced voltage profile to create a robust and flexible distribution network.

1. Introduction

The amount of electrical energy consumers require is snowballing, spurred by new electrical and electronic appliances. All categories of the consumer class, such as residential, commercial, and industrial participated in energy growth due to the growth in electric vehicles and other intelligent devices based on the consumption of electrical energy. In addition to being a necessary part of society, the electrical power distribution industry's job is critical, because it is dependent on upstream power resources and needs to provide an adequate supply to all classes of customers with high-quality power without interruptions. The electricity grid is rapidly growing, delivering reliable, and affordable electricity to everyone by predicting the level of load demand, which changes and fluctuates continuously. The COVID-19 pandemic continues to have a significant impact on the world's energy systems. In this scenario, the modest decline in energy demand caused by direct limitations on industry, commerce, and other activities, and the general economic slump have disproportionately affected the power sector [1]. This article analysed the influence of the COVID-19 pandemic lockdown on demand, operation, and supply in the Indian power system [2]. In addition, as shown in Figure 1, an unusual situation in load demand seen due to the COVID-19 epidemic has significantly impacted the

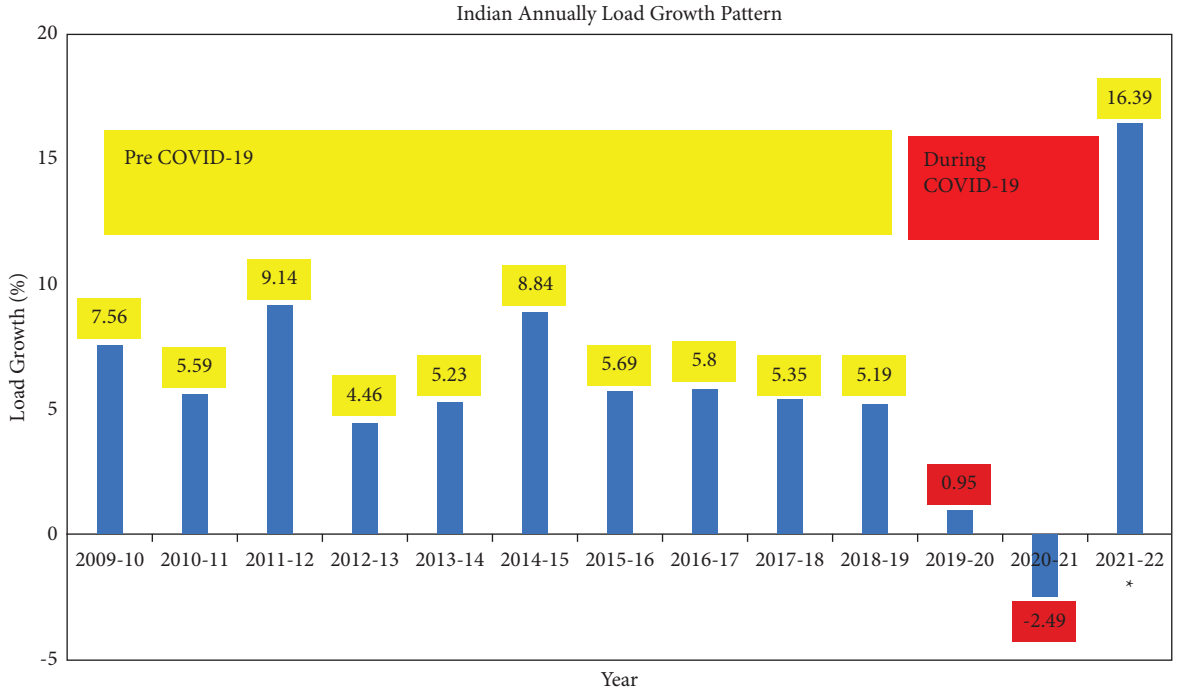

Figure 1: Load growth pattern of India.

energy consumption and trajectory of India. As a result, load demand scenarios are critical for comprehensive knowledge of the distribution network and system operation, planning, and long-term strategy. This article suggests the significant penetration of DG into the distribution network for the development of defence mechanisms meant to improve the grid's resiliency against COVID-19-type incidents [3].

The main components of the power system are the power generation plant, transmission system, and distribution system (DS). They form the value chain of power delivery to the consumer [4]. DS is the most important part of the value chain because it is exposed to failure and disturbance caused by the consumer side as well as the generation and transmission side. The power loss in the DS is much higher than in the transmission system because of the extreme R/X ratio and a major portion of investment is allocated to the DS of the total electrical industry. The voltage profile of DS is affected by load uncertainty due to the highly nonlinear characteristics of the load. The poor voltage stability could lead to a total shutdown of the DS. The reactive power unbalance in the DS severely affects its performance while delivering power to the consumer. A large fluctuation in reactive power introduces harmonics that will degrade the quality of power and the chances of voltage collapse will increase. Load demand volatility may be addressed by providing sufficient assistance through DG and DSTATCOM (DGDST).

Integration of DGDST changes DS's characteristics from passive to active with multidirectional power flow [5]. It will make DS ill-conditioned by having negative impacts. These include reverse power flow and unaccepted voltage levels, combined with high active power loss (APL) and reactive power loss (RPL) if the DGDST location and size are nonoptimal. Therefore, an optimal solution consisting of the location and size of DGDST obliges us to overcome the negative impacts and achieve the positive effects by maintaining necessary constraints within their tolerable limits for practical load demand. Integration of DGDST makes the DS more resilient to any unhealthy situation on the grid. It also enhances the efficiency of DS by depreciating the power loss and increasing the voltage stability.

DS can be categorized based on different structures defined in the power system: radial balance distribution system (RDS), radial unbalanced distribution system (RUDS), mesh distribution system, etc. The DS is an intrinsically unbalanced system due to serving single and three-phase loads via a distribution transformer. The loads in each phase are unequal. Distribution lines are not transposed like transmission lines. There are already many researchers analyzing RDS to enhance the performance of DS by means of integration of DGDST [6]. Generally, the constant load is taken for the analysis of DS, but practically, different types of load are served by DS, including residential load, industrial load, and commercial load; so there is a need for a mixed load demand that consists of all types of load with a suitable participation factor [7]. In the presented work, RUDS have been considered for the integration of DGDST individuals and simultaneously to enhance the performance of a new mixed load model. DGs are power-generating units usually integrated into DS to decrease power loss and maximize the voltage profile to ensure secure and reliable delivery. It is becoming popular because it avoids the need for new distribution lines near the end user and prevents new transmission lines in the middle part of the value chain. That makes it an economical and adopted solution for DS [8]. Nowadays, DGs with renewable energy

sources, like PV and wind-based DGs, etc., strengthen the concept of DG installation due to its environmental concern by decreasing carbon emissions [8]. Mostly, loads are inductive in nature, which causes an unbalance in reactive power. DSTATCOM is the promising solution for steady-state reactive power compensation in DS by absorbing both active and reactive power by inserting a voltage of inconstant magnitude and phase angle at the point of coupling connection in DS. It will maintain the voltage within permissible limits and increase the stability of the system [9]. Since DGs with a nonunity power factor can also inject necessary reactive power into DS for compensation of unbalancing of reactive power, it will be an uneconomical solution because of the higher cost of DG and minimum regulation in voltage compared with the DSTATCOM support system. Optimal allocation of DGDST can provide several technical and economic advantages. It minimizes the APL, and RPL and maximizes the voltage stability. The improved voltage profile (IVP), lower branch current, improved power quality, and increased trustworthiness of the DS attained afterward integration of DGDST [10].

Very little research has been described for the planning of DGDST in RUDS. The power loss is lessened by the placement of DG using the voltage index method and sizing computed by the variation technique algorithm. The size should not be greater than 20% of the feeder loading in RUDS with voltage-dependent LM; it is a combination of constant power, constant current, and constant impedance loads [10]. To compensate for reactive power, a multishunt capacitor is allocated optimally using hybrid particle swarm optimization considering harmonics. The problem was developed as a nonlinear integer programming problem with inequality constraints [11]. Optimal capacitor placement is executed using a simulated annealing technique, including a greedy search technique to make a balance between the quality of solution and computational speed in a substantial practical scale distribution system considering different load level peaks [12]. Reverse power flow constraints are incorporated for the optimal location of solar-based DGs in practical RUDS. It gives criteria for limiting the maximum optimal size of DG. The size of DG and DSTATCOM should be according to the loading at each phase. An equal rating of DGDST is not preferable as it increases reactive power loading and energy saving. The optimal size and location of both DG and KVAR support are determined using particle swarm optimization (PSO) by minimizing losses in RUDS [13]. The voltage profile is better when an unequal size of KVAR support is provided in each phase compared to the rating of the same size. Various metaheuristic techniques (GA, PSO, and BSFLA-PRTPLF) were implemented to allocate biomass-based DG in RUDS, including a probabilistic load model to enhance the voltage profile with desirable voltage limits on all load buses [14]. Simultaneously optimization for phase balancing by providing the required complex power and size of conductor for RUDS using a differential evolution (DE) algorithm results in significant improvement in power loss and a drop in voltage [15].

Because of the recent COVID-19 pandemic, energy demand has been lowered drastically. This pandemic increased demand for residential loads due to changed habits around the world, as people typically stay home and work from home, if possible, although there is a significant decrease in commercial and industrial loads because governments worldwide have been forced to limit business activity in response to reducing the threat of coronavirus [16]. This catastrophic situation poses new challenges for the technological and financial operations of the power sector [17]. Technically, the distribution industry suffered from negative and positive load growth subsequent to voltage infringement and was economically weak due to a substantial decline in demand for industrial and commercial loads despite having surplus electricity generation from renewable and nonrenewable sources [18]. Therefore, most electrical utilities worldwide have launched an emergency recovery initiative to resolve these current problems and risks. The changed situation during COVID-19 created a greater need for DG allocation because upstream electricity from traditional power plants was disturbed. Therefore, the purpose of this analysis includes the investigation into the DG allocation considering scenarios during COVID-19, accompanied by the never-seen load growth challenges confronted by EDS. As the impact of COVID-19 increased, all countries worldwide imposed a lockdown. The electrical industry was also affected due to the lockdown by the shutdown of factories and commercial activities, so the power demand decreased. However, the generation of electricity remained at peak demand since electricity storage is not possible, so this imbalance in power became large and uneconomical because most of the revenue comes from prime consumers (industrial and commercial). Many governments have imposed a "lockdown" on their citizens to reduce communal spread, which affects the energy sector. In this context, this paper [19] examines COVID-19's impact on the global energy market, especially in India, and describes the operation of different countries and how they secured their power sector throughout the pandemic. In a lockdown, people stayed at home, so residential demand increased. It created a change in LM, which caused a steep fall in load demand, and created a stability problem, which made it a challenging task to operate DS [20].

COVID-19's crisis and lockdown constraints have lowered activities and energy use. Commercial and public administration operations have increased energy consumption, and the residential sector has gained scale economies [21]. For the COVID-19 situation, a new LM equation was adopted due to changes in different loading share types in active and reactive power loading. In critical situations like lockdown due to COVID-19, the demand varies according to load type. Residential demand increases, whereas commercial and industrial demand decreases, and battery charge loading and other loading are also affected proportionally. All the changes made in the load weighting factor are assumed by analyzing the report on the electrical industry's first response to COVID-19 for different electrical systems [22]. The peak load demand of the Indian power sector is varied, as shown in Figure 2. The fluctuation in peak

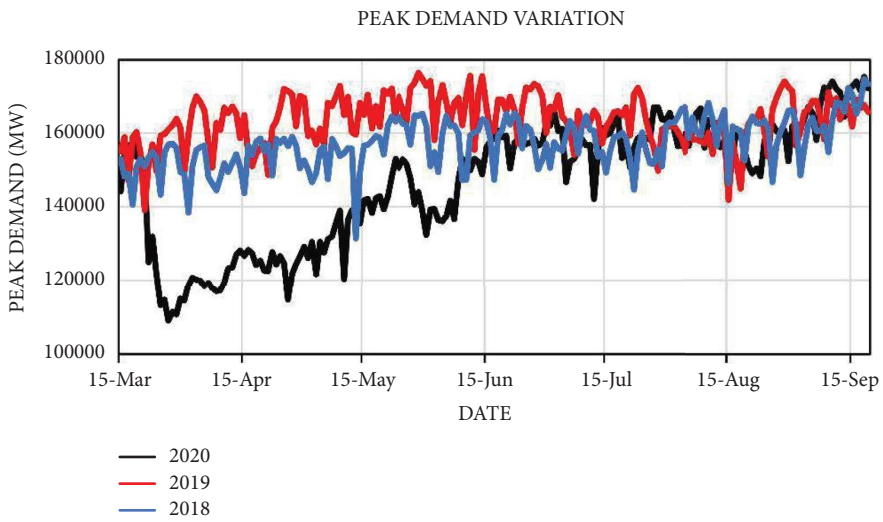

Figure 2: Peak demand variation of India.

load demand causes energy fluctuation of the power network depicted in Figure 3. The paper gives officials a more detailed idea of the pandemic's influence on electricity demand to minimize losses [23].

From the literature review, it has been found that the optimal allocation problem of DG as well as DSTATCOM is solved by various researchers using both deterministic and stochastic approaches using sensitivity analysis and metaheuristic optimization algorithms [24, 25]. In the optimization field, there are so many algorithms based on the metaphor of the behavior of animals, fishes, insects, or any natural phenomenon. It is ambiguous to select one algorithm for an optimization problem by tuning the decision variable with an algorithm-specific parameter to get the best result. To overcome this issue, a new metaphor-less Rao optimization algorithm is taken for minimizing the objective function [26]. A proposed optimization algorithm has been employed in the multiobjective optimization of selected thermodynamic cycles [27]. The multiobjective function is formulated by assigning suitable weight to every objective function based on the priority of DS [28]. The problem of DSTATCOM allocation is given less attention compared to DG allocation for RUDS since a reactive power support capacitor is installed in the DS, but with the invention of power electronics devices, DSTATCOM is a better option for mitigating issues related to reactive power imbalance. Simultaneous allocation of DGDST is very rare for RUDS, whereas in BRDS many studies have been found for single and multiple allocations of DGDST [29]. In [30, 31], DGs are modelled as PV nodes delivering real power at unity power factor are taken for URDN analysis. Although DSTATCOM's primary role is to provide reactive power (as required) to the PCC-modelled voltage control system, it is modelled as a constant source of reactive power to provide adequate support for reactive power compensation [32, 33].

During COVID-19, electric utilities implemented various sorts of resilience thinking towards power system resilience through decision-making processes [34]. Installation of DGDST will convert DS into a smart distribution system (SDS) for unpredicted fluctuations in load demand caused by any emergency situation like the COVID-19 pandemic.

The literature review suggests the following research gap:

(i) The load demand from a different class of consumers plays a vital role in determining the existing EDS performance by incorporating DG. Most of the research work followed a constant power load model for DS analysis. However, little work has been carried out to modify the practical LM based on residential, commercial, and industrial load types only. In the proposed work, LM is composed by aggregating the load demand raised by the different classes of consumers, including battery charges and other residual loads, to analyze the DS that was not considered before.

(ii) From the literature, it is learned that metaheuristic optimization provides more accurate and reliable outcomes with lower computational time than sensitivity-based and classical optimization methods due to certain advantages. The optimal allocation of DG in EDS is a nonlinear optimization problem, and there is continuous scope for improving the optimal solution with fewer complicated approach in a minimum time with reasonable accuracy.

(iii) COVID-19 worldwide affected the energy sector. The EDS was affected due to the lockdown declared, resulting in an imbalance between supply and demand from various LM. From the literature, it is revealed that DG installation enhances the capability of EDS to meet the increased demand for the load. Therefore, it is vital to analyze the consequences of COVID-19 for DG allocation designed for positive and negative growth in load demand by various LM.

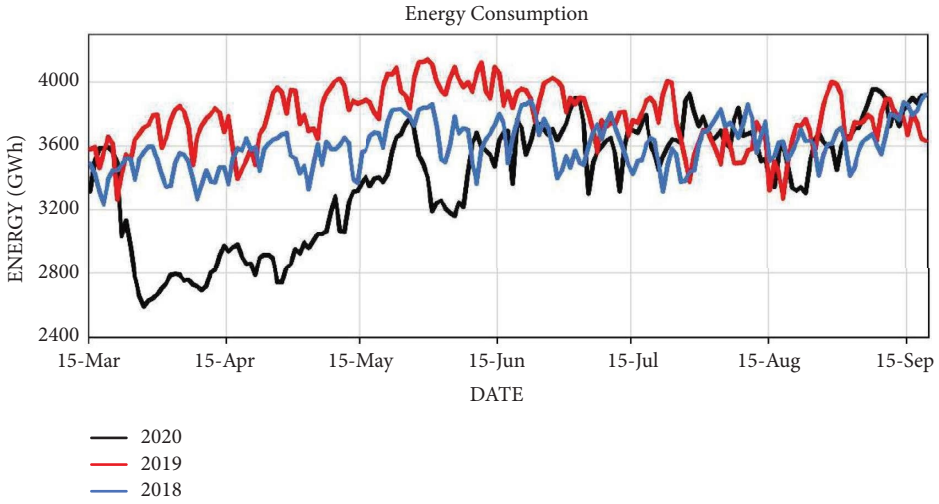

Figure 3: Energy consumption of India.

The main contribution to this work can be summarized as follows:

(i) The effect of COVID-19 is taken to analyze the DS and its impact is balanced by DGDST allocation in lockdown duration

(ii) A new mixed load model has been formulated for performance analysis of RUDS

(iii) A multiobjective function consists of APL, RPL, MVV, and VSI, which is considered a minimization problem

(iv) Simultaneous allocation of multiple DG and DSTATCOM in URDS is performed separately following successive allocation of one, two, and three DG and DSTATCOM to minimize multiobjective function

(v) A new Rao metaheuristic optimization free from a metaphor-based hypothesis is proposed to resolve the enigma of DGDST allocation

The remaining paper is organized as follows. In Sections 2–4 the detailed structure of the problem formulation is given, including objective function and load flow analysis. The load flow for the test system is provided in Section 5. Section 6 presents an overview of the Rao optimization algorithm, followed by applying the proposed algorithm to the DGDST optimal allocation problem. Simulation results were discussed briefly in Section 7. Eventually, the conclusion and future scope of the proposed work are given in Section 8.

2. Load Models (LMs)

Earlier, most of the research work was carried out with a constant load model, but DS cannot be subjected to a single load model characteristic that will optimize the system for all types of installation of DGDST. The load deterministic modelled according to different LMs by using exponential load components for active and reactive power load values is shown in Table 1 [35]. The weightage of load components is taken from [28, 36]. In this work, along with the constant load model, a new mixed load model is considered for the optimization problem of DGDST allocation. In many cases, the load demand characteristics of the distribution system are determined by the constant load.

2.1. Constant LMs. A mathematical equation has been developed for load flow analysis to compute load demand according to the load type. Furthermore, the optimal allocation of DG is carried out based on the characteristics of each load. The loads are not constant in actuality, so all types of loads, residential, commercial, industrial, battery charge, and remaining loads are considered. The remaining load types include all the ignored loads that are not covered by any type of load to cover the maximum span of loading. That will make the load equation more realistic for analysis of DS in a realistic manner, like agriculture load. The constant load model is formulated as a function of nominal voltage and bus voltage raised by the power exponent given by the following equations:

$$P = P_{Oj}\left(\frac{V_j}{V_o}\right)^{Cpo},$$
$$Q = Q_{Oj}\left(\frac{V_j}{V_o}\right)^{Cqo}, \quad (1)$$

where P is the active power load, P_{Oj} nominal active power load, Q is the reactive power load, Q_{Oj} is the nominal reactive power load, V_j is the operating voltage for the constant load, V_o is the nominal voltage, and C_{po} and C_{qo} are the load exponential coefficient of active and reactive power for the constant load, respectively

It is a voltage-independent model. Any change in voltage magnitude will not affect system demand, so it remains constant irrespective of any change in voltage.

Table 1: The value of exponential factor.

Load type	P exponent	Value	Q exponent	Value
Constant	Cpo	0	Cqo	0
Residential	Rpo	0.92	Rqo	4.04
Commercial	$CMpo$	1.51	$CMqo$	3.4
Industrial	Ipo	0.18	Iqo	6
Battery charge	Bpo	2.59	Bqo	4.06
Another load	$OTpo$	1.3	$OTqo$	4.3

2.2. Mixed LMs. In practical situations, loads are not constant, since DS is dependent on consumer mix, providing power to different types of load according to their active and reactive demand, so loads are a combination of unique types of load demand, for instance, residential, industrial, and commercial [37]. The mixed load is composed by taking different weightage of all types of load. The historical trend of different classes of consumers in India is utilized to formulate a new mix load demand model equation. The weighting components-based load modelling is adopted. Mixed load analysis is also carried out using a different weighting factor for each load depending upon the impact. The weighting factor is decided by the consumption of active and reactive power by the various types of load given in Table 2, so total active and reactive demand is distributed as follows:

$$\begin{aligned} P_{\mathrm{MIX}} &= P_{Oj}\left(K_R\left(\frac{V_j}{V_o}\right)^{Rpo} + K_{CM}\left(\frac{V_j}{V_o}\right)^{CMpo} + K_I\left(\frac{V_j}{V_o}\right)^{Ipo} + K_B\left(\frac{V_j}{V_o}\right)^{Bpo} + K_{OT}\left(\frac{V_j}{V_o}\right)^{OTpo}\right), \\ Q_{\mathrm{MIX}} &= Q_{Oj}\left(K_R\left(\frac{V_j}{V_o}\right)^{Rqo} + K_{CM}\left(\frac{V_j}{V_o}\right)^{CMqo} + K_I\left(\frac{V_j}{V_o}\right)^{Iqo} + K_B\left(\frac{V_j}{V_o}\right)^{Bqo} + K_{OT}\left(\frac{V_j}{V_o}\right)^{OTqo}\right), \end{aligned} \tag{2}$$

where P_{MIX} and Q_{MIX} are active and reactive power for the mixed load, respectively, and K_R, K_{CM}, K_I, K_B, and K_{OT} are the weighting factors for residential, commercial, industrial, battery charge, and the other load, respectively.

The mixed load model is voltage dependent. Any deviation in voltage will be caused by specific types of load exponents that will give corresponding active and reactive power demand. That will change the steady state condition of the DS. Therefore, the mixed model will give an actual estimate of all the DS parameters for load flow analysis and further investigation.

3. LM during COVID-19

The coronavirus has triggered widespread devastation; a major casualty is the power sector. During the COVID-19 pandemic, many countries imposed a nationwide lockdown. Electrical DS was affected by it because of the shutdown of factories and industries. There was a huge plunge in electrical demand from industrial and commercial users, whereas due to people staying in homes, the residential demand was high [30]. The demand growth is decreased by the lockdown and makes the distribution sector vulnerable. The power shared by residential consumers is higher than industrial, commercial, and other types of consumers [38]. A major portion of revenue comes from industrial and commercial customers for DISCOM. A reduction in demand could lead to a huge loss of revenue. For the COVID-19 situation, new load model equations have been adopted due to changes in different types of loading share in active and reactive power loading to analyze practical load uncertainty. In this present work, the impact of this situation is shown by modifying the weighting component of individual load and further finding a new solution for optimal allocation of DGDST during the lockdown. Table 2 presented the value of the weighting factor [22].

4. Problem Interpretation

In this section, problem formulation and load flow are addressed. An objective function has been developed, which will be adopted for the optimal allocation of DGDST in optimization problems relating to the proposed optimization algorithm. Figure 4 presented the general description of an unbalanced distribution system.

4.1. Active Power Loss (APL). In DS, the R/X ratio is high and, due to its radial construction, there is a huge loss of active power. To augment the capability of DS, the primary objective is to reduce its APL, which will maximize the performance of DS. The APL is determined using the branch current loss formula given by the following equations:

$$\begin{aligned} P^b_{Loss,br(xy)} &= \mathrm{Real}\left\{\left(V^b_x - V^b_y\right)\left(I^b_{xy}\right)^*\right\}, \\ P^a_{Loss,br(xy)} &= \mathrm{Real}\left\{\left(V^a_x - V^a_y\right)\left(I^a_{xy}\right)^*\right\}, \\ P^c_{Loss,br(xy)} &= \mathrm{Real}\left\{\left(V^c_x - V^c_y\right)\left(I^c_{xy}\right)^*\right\}, \end{aligned} \tag{3}$$

where $P^a_{Loss,br(xy)}$, $P^b_{Loss,br(xy)}$, and $P^c_{Loss,br(xy)}$ represent the active power losses in distinct branches for phase "a", "b,"

Table 2: The value of weighting factor.

Load multiplier	Pre COVID-19	During COVID-19	Demand Status (%)
K_R	0.25	0.55	54.54 (+)
K_{CM}	0.1	0.06	40 (−)
K_I	0.42	0.24	42.8 (−)
K_B	0.05	0.03	40 (−)
K_{OT}	0.18	0.12	33.3 (−)

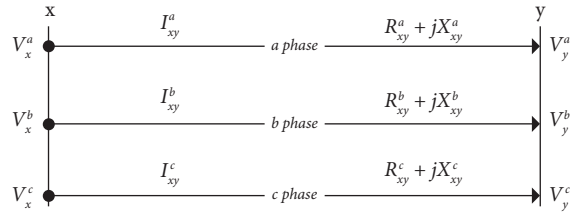

Figure 4: General description of unbalanced distribution system.

and "*c*," respectively. The total APL is determined by the summation of all phase losses of distributed line, given by the following equation:

$$\mathrm{APL} = P^T_{Loss} = \sum\left(P^a_{Loss,br(xy)} + P^a_{Loss,br(xy)} + P^a_{Loss,br(xy)}\right). \tag{4}$$

So the first objective function is subjected to minimization of the total APL of the DS.

$$F_1 = \min\ (\mathrm{APL}). \tag{5}$$

4.2. Reactive Power Loss (RPL). The large amount of RPL in the DS causes instability and fluctuation in voltage, which results in system collapse. For the smooth operation of the DS, the reactive power loss (RPL) should be minimized. That will make the DS more resilient to any unhealthy situation. The reactive power loss is determined using the branch current loss formula given by the following equations:

$$\begin{aligned} Q^a_{Loss,br(xy)} &= \mathrm{Im}g\left\{\left(V^a_x - V^a_y\right)\left(I^a_{xy}\right)^*\right\}, \\ Q^b_{Loss,br(xy)} &= \mathrm{Im}g\left\{\left(V^b_x - V^b_y\right)\left(I^b_{xy}\right)^*\right\}, \\ Q^c_{Loss,br(xy)} &= \mathrm{Im}g\left\{\left(V^c_x - V^c_y\right)\left(I^c_{xy}\right)^*\right\}, \end{aligned} \tag{6}$$

where $Q^a_{Loss,br(xy)}$, $Q^b_{Loss,br(xy)}$, and $Q^c_{Loss,br(xy)}$ represent the reactive power losses in distinct branches for phase "*a*", "*b*," and "*c*," respectively. The total RPL is determined by the summation of all phase losses of the distributed line, given by equation (5).

$$F_2 = \min\ (\mathrm{RPL}). \tag{7}$$

Hence, the second objective function is subjected to minimization of total RPL of the DS.

4.3. Minimum Value of Voltage (MVV). It is the minimum value of voltage (MVV) among all the buses in the DS. The MVV is important for the system stability of the DS. The lower magnitude of MVV indicates a high probability of system reliability, whereas its value close to the reference value indicates the better reliability of DS with less probability of system collapse.

$$\begin{aligned} \mathrm{MVV}^a &= \min\left\{V^a_1, V^a_2 \ldots\ldots\ldots\ldots V^a_{n-1}, V^a_n\right\}, \\ \mathrm{MVV}^b &= \min\left\{V^b_1, V^b_2 \ldots\ldots\ldots\ldots V^b_{n-1}, V^b_n\right\}, \\ \mathrm{MVV}^c &= \min\left\{V^c_1, V^c_2 \ldots\ldots\ldots\ldots V^c_{n-1}, V^c_n\right\}, \end{aligned} \tag{8}$$

where MVV^a, MVV^b, *and* MVV^c represent the MVV in distinct branches for phase "*a*", "*b*," and "c," respectively. The total RPL is determined by the summation of all phase losses of the distributed line, given by the following equation:

$$\mathrm{MVV}^T = \sum\left(\mathrm{MVV}^a + \mathrm{MVV}^b + \mathrm{MVV}^c\right). \tag{9}$$

So the third objective function is subjected to maximization of the minimum voltage magnitude of the distribution system.

$$F_3 = \max\left(\mathrm{MVV}^T\right). \tag{10}$$

4.4. Voltage Stability Index (VSI). It is defined as the capability of the DS to maintain the voltage within a permissible range. The zero value of VSI indicates the voltage collapse, whereas it becomes unity for a healthy DS. It is calculated by the following equation.

$$\begin{aligned} \mathrm{VSI}^a_y &= U^{a4}_x - 4\left(P^a_y R^a_{xy} + Q^a_y X^a_{xy}\right)U^{a2}_x - 4\left(P^a_y X^a_{xy} - Q^a_y R^a_{xy}\right), \\ \mathrm{VSI}^b_y &= U^{b4}_x - 4\left(P^b_y R^b_{xy} + Q^b_y X^b_{xy}\right)U^{b2}_x - 4\left(P^b_y X^b_{xy} - Q^b_y R^b_{xy}\right), \\ \mathrm{VSI}^c_y &= U^{c4}_x - 4\left(P^c_y R^c_{xy} + Q^c_y X^c_{xy}\right)U^{c2}_x - 4\left(P^c_y X^c_{xy} - Q^c_y R^c_{xy}\right), \end{aligned} \tag{11}$$

where VSI^a_y,VSI^b_y,*and*VSI^c_y are phasewise voltage stability index of receiving bus *y*. P_y, and Q_y are active and reactive power of bus *y*. R_{xy}, *and* X_{xy} are resistance and reactance between buses *x* and *y*.

The VSI is determined for each phase and the minimum value of the VSI is summed up for maximization.

$$\mathrm{VSI}^T = \sum\left(\mathrm{VSI}^a_{\min} + \mathrm{VSI}^b_{\min} + \mathrm{VSI}^c_{\min}\right). \tag{12}$$

Hence, the fourth objective function is subjected to maximization of the minimum voltage stability index magnitude of the DS.

$$F_4 = \max\left(\mathrm{VSI}^T\right). \tag{13}$$

4.5. Overall Objective Function. The objective function of the problem is to find the optimal location and sizing of DG and DSTATCOM individually and together that will reduce the APL and RPL and maximize the MVV and VSI. The single objective function optimization problem is converted to a multi-objective function using suitable weighting factors for every single objective depending upon priority is formulated as

$$\mathrm{OF} = (w_1 \times F_1) + (w_2 \times F_2) + \left(w_3 \times \frac{1}{F_3}\right) + \left(w_4 \times \frac{1}{F_4}\right). \tag{14}$$

Such that

$$\sum_{i=1}^{4} w_i = 1, \tag{15}$$

where w is the weighting factor.

Now, the minimization of the multiobjective function is an optimization problem.

4.6. System Constraints. These constraints are checked in every iteration for the feasible solution according to the requirements of the DG and DSTATCOM allocation optimization problems. The developed multiobjective function is subjected to the following equality and inequality constraints as follows.

4.6.1. Equality Constraints. The algebraic sum of the power in the electrical distribution network and loss should be identical to the power delivered by the DG and DSTATCOM. Since the nonoptimal allocation of DG and DSTATCOM could affect the operation of DS, that condition is restricted by applying the following constraint:

$$\begin{aligned} P_{Loss} + \sum_{l=1}^{Nl} P_D &= \sum_{i=1}^{\mathrm{NDG}} P_{DGi}, \\ Q_{Loss} + \sum_{l=1}^{Nl} Q_D &= \sum_{i=1}^{\mathrm{NDG}} Q_{DSTi}, \end{aligned} \tag{16}$$

where P_D active power demand raised by the load, Nl total number of distribution lines, NDG number of DG, P_{DG} active power injected by DG, Q_D reactive power demand raised by the load, Q_{DST} reactive power injected by DSTATCOM.

4.6.2. Inequality Constraints

(1) Voltage Magnitude Constraint. The voltage magnitude after each iteration should be within the tolerance limit; otherwise, it will lead to a problem of unbalancing in voltage magnitudes, since there is a large fluctuation in bus voltage, and then it will inject a higher amount of current through the branches. That would make the solution nonoptimal.

$$V_{\mathrm{bus}}^{\min} \le V_{\mathrm{bus}} \le V_{\mathrm{bus}}^{\max}. \tag{17}$$

(2) DG Size Constraint. The power injected by DG should be within the described limits so that we can operate DS consequently. The power supplied by DG is controlled by real power constraints.

$$P_{\mathrm{DG}}^{\min} \le P_{\mathrm{DG}} \le P_{\mathrm{DG}}^{\max}. \tag{18}$$

(3) DSTATCOM Size Constraint. The power supplied through DSTATCOM should be within reasonable limits for the efficient functioning of DS. The power supplied by it is controlled by reactive power constraints.

$$Q_{\mathrm{DST}}^{\min} \le Q_{\mathrm{DST}} \le Q_{\mathrm{DST}}^{\max}. \tag{19}$$

(4) Line Loading Constraint. The line loading should not be greater than the maximum permissible limit, and it creates a line outage due to excessive power flow. In this work, several types of load are taken, so it is worth considering line loading constraints to find the optimal solution.

$$S \le S^{\max}, \tag{20}$$

where $S^{\max}$ is the maximum loading on the line connected between two buses, it is the maximum power transfer capability of that line.

5. Load Flow with DG and DSTATCOM

The load flow method for RUDS shown in Figure 5 is occupied from [39]. It is composed of the multiplication of two matrices. The first is the bus injection to a branch-current matrix (BIBC) and the other is the branch current to bus voltage matrix (BCBV). The relationship calculations are given for phase a as follows:

$$[B_a] = [BIBC_a][I_a], \tag{21}$$

where I_a and B_a are the branch currents and equivalent current injection vector for phase a,

$$[\Delta V_a] = [BCBV_a][B_a], \tag{22}$$

ΔV_a is the difference between bus voltage and substation voltage for phase a. Bus voltage is a function of current flowing in branches and the voltage of DS along with network parameters.

Now, from equations (21) and (22),

$$[\Delta V_a] = [\mathrm{BCBV}_a][\mathrm{BIBC}_a][I_a], \tag{23}$$

$$[\mathrm{DLF}_a] = [\mathrm{BCBV}_a][\mathrm{BIBC}_a], \tag{24}$$

DLF_a is the direct load flow matrix for phase a. The relation between bus voltage and equivalent current injections of buses for phase a can be given as

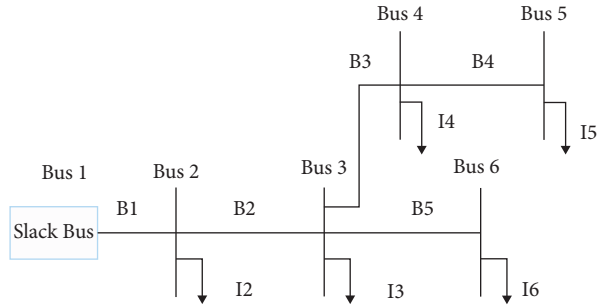

Figure 5: 6-bus radial distribution system.

$$[\Delta V_a] = [\mathrm{DLF}_a][I_a]. \tag{25}$$

In RUDS, there will be three conductors, so all the equations are similarly derived for phases b and c. The solution to load flow is found by using the following iterative formulas.

$$\begin{aligned} I_{i,a}^{k} &= \left(\frac{P_{i,a} + jQ_{i,a}}{V_{i,a}^{k}}\right)^{*}, \\ \left[\Delta V_{a,i}^{k+1}\right] &= \left[\mathrm{DLF}_a\right]\left[I_{a,i}^{k}\right], \\ \left[V_{a,i}^{k+1}\right] &= \left[V^{0}\right] + \left[\Delta V_{a,i}^{k+1}\right], \end{aligned} \tag{26}$$

$I^{k}_{a,i}$is equivalent current injection for phase a, ith bus during the kth repetition. $V^{k}_{a,i}$ is the voltage of phase a, ith bus in the kth repetition. $P_{i,a} + jQ_{i,a}$ is complex power for phase a, ith bus is determined as follows:

$$P_{i,a} + jQ_{i,a} = \left(P_{iD,a} - P_{iG,a}\right) + j\left(Q_{iD,a} - Q_{i,G,a}\right), \tag{27}$$

$P_{iD,a} + jQ_{iD,a}$ is the total demand of the DS for phase a. $P_{iG,a} + jQ_{iG,a}$ is the total generation for DS for phase a.

A DG with unity power factor (UPF) is taken as a source to provide adequate active power into DS, whereas DSTATCOM is modelled as a source to provide reactive power. The change in complex power will modify the current of "equation (24)."

$$\mathrm{DG}_s \in [P_{DG}, Q_{DG}] \quad \mathrm{DG}_{l,d} \in N_{\mathrm{Bus}} \quad d = 1, 2, 3 \ldots\ldots\ldots\ldots N_{DG}, \tag{28}$$

where s is the size of DG, l is the location of DG, and d is the dimension of DG $d = 1, 2, 3$.

$$\begin{aligned} c &= \tan\left(\cos^{-1}\left(\mathrm{PF}_{DG}\right)\right), \\ Q_{DG} &= c \times P_{DG}, \end{aligned} \tag{29}$$

where c is a conversion coefficient, PF_{DG} power factor of DG unit.

In this work DG with unity power factor (UPF) $\mathrm{PF}_{DG} = 1$ p.u.

The new modifying current with DG is given by the following equation:

$$I_{i,a,DG}^{k} = \left(\frac{P_{i,a} - P_{i,a,DG} + jQ_{i,a} - Q_{i,a,DSTATCOM}}{V_{i,a}^{k}}\right)^{*}, \tag{30}$$

$Q_{i,a,\mathrm{DSTATCOM}}$ is the reactive power provided by DSTATCOM, it is given by [34], according to the following equation:

$$\begin{aligned} jQ_{i,a,DSTATCOM} &= \left(V_{i,a,DSTATCOM}\angle\theta_{i,a,DSTATCOM}\right). \\ &\left(I_{i,a,DSTATCOM}\angle\frac{\pi}{2}\theta_{i,a,DSTATCOM}\right). \end{aligned} \tag{31}$$

DSTATCOM's transformed voltage and inserted reactive power are used for continued forward sweep to evaluate load currents in the next iteration of backward sweep load flow. The iterative formulas will be modified according to the voltage magnitude injected by DSTATCOM as followed:-

$$\begin{aligned} \left[V_{a,i}^{k+1}\right] &= \left[V^{0}\right] + \left[\Delta V_{a,i}^{k+1}\right] + \left[V_{i,a,DSTATCOM}\right], \\ I_{i,a,\mathrm{DST}}^{k} &= \left(\frac{P_{i,a} + j\left(Q_{i,a} - Q_{i,a,DSTATCOM}\right)}{V_{i,a}^{k}}\right)^{*}, \end{aligned} \tag{32}$$

where $I^{k}_{i,a,\mathrm{DST}}$ is the updated current after integration of DSTATCOM in the DS. Now, with the installation of DGDST, the new iterative current is modified according to the following equation.

$$I_{i,a,\mathrm{DGDST}}^{k} = \left(\frac{\left(P_{i,a} - P_{i,a,DG}\right) + j\left(Q_{i,a} - Q_{i,a,DSTATCOM}\right)}{V_{i,a}^{k}}\right)^{*}, \tag{33}$$

where $I^{k}_{i,a,\mathrm{DGDST}}$ is the updated current after integration of DG and DSTATCOM in the DS. If the power factor of DG is unity, then the modified term is given by "equation (27)."

$$I^{k}_{i,a,\mathrm{DGDST}} = \left(\frac{\left(P_{i,a} - P_{i,a,DG}\right) + j\left(Q_{i,a} - Q_{i,a,DSTATCOM}\right)}{V^{k}_{i,a}} \right)^{*}. \tag{34}$$

The numerator of equation (30) is decreased owing to DG's active power and reactive power injected through DSTATCOM. The denominator increases due to the injection of DSTATCOM voltage, hence leading to an increase in the voltage of DS and lower power loss.

6. Rao Algorithm

There are various metaphor-based optimization algorithms for optimization. However, from the effectiveness point of view, all techniques are not perfect or give an unreliable solution; the computational time is also high. That is why, to solve complex problems with accuracy, there is a necessity for metaphor-less optimization algorithms [26]. It is an uncomplicated concept without the fine-tuning of artificial particles that will make implementation more straightforward than conventional metaphor-based techniques. The algorithm was successfully implemented for multiobjective engineering optimization, which showed promising results [27].

The benefits of the Rao algorithm are as follows:

(1) It uses no metaphor for the optimization of multiobjective problems, which makes it superior

(2) In this algorithm, the best and worst solutions amid optimization of a given problem are obtained, and interactions occur randomly between the candidate solutions

(3) It necessitates general control parameters like population size and iteration numbers; no other algorithm-specific parameters are involved

(4) It has already been tested on various dimensions' benchmark functions with constrained and multimodeling properties, which proves the attractiveness of adopting this algorithm for different optimization problems

First of all, initialize the initial population to minimize the OF. If m number of decision variables are there and n number of possible solutions for any iteration i. In the optimization process, let the best agent attain the OF's best value in the whole search space with all possible solutions. Similarly, the worst agent obtains the OF's worst value.

If $X_{j,\ k,\ i}$ is the value of decision variable X for the jth variable during the ith iteration for the kth agent. The magnitude is going to change according to the following equations:

$$X'_{j,k,i} = X_{j,k,i} + r_{1,j,i} * \left(X_{j,best,i} - X_{j,worst,i}\right), \tag{35}$$

$$X'_{j,k,i} = X_{j,k,i} + r_{1,j,i} * \left(X_{j,best,i} - X_{j,worst,i}\right) + r_{2,j,i} * \left(\left|X_{j,k,i} or X_{j,l,i}\right| - \left|X_{j,l,i} or X_{j,k,i}\right|\right), \tag{36}$$

$$X'_{j,k,i} = X_{j,k,i} + r_{1,j,i} * \left(X_{j,best,i} - X_{j,worst,i}\right) + r_{2,j,i} * \left(\left|X_{j,k,i} or X_{j,l,i}\right| - \left(\left|X_{j,l,i} or X_{j,k,i}\right|\right)\right), \tag{37}$$

where $X_{j,\mathrm{best},i}$ is the value of the variable j for the best candidate and $X_{j,\mathrm{worst},i}$ is the variable j for the worst candidate during the ithiteration. $X'_{j,k,i}$ is the updated value of $X_{j,k,i}$ and $r1_{,j,i}$is random number for the $_j$th variable during the $_i$th iteration in the range [0, 1].

The value of the decision variable is compared with a randomly selected agent solution. According to the fitness function, information is exchanged according to equations (35)–(37).

The decision variable value will be updated according to the fitness of the OF. If the previous solution was superior to the current solution, then the agents' value would be replaced with a better OF value in the current solution. If the current solution is more promising than the previous solution, then the agent's value will be replaced by the previous solution. So the loop will continue until convergence criteria are not attained; it may be the maximum number of iterations or any other tolerance or mismatching criteria according to the problem. In this paper, the Rao algorithm is implemented on the DG optimization problem with 50 populations and 100 iterations. Convergence characteristics are plotted for various LMs that show the best, worst, and average results, respectively, after several independent runs. The flow chart is given in Figure 6. The convergence characteristics for formulated problems are drawn for different distinct cases shown in Figure 7.

The optimal value of the objective function is obtained after 100 runs. The results with minimum objective values are selected for the convergence curve under three different settings of the proposed algorithm with 50, 100, and 150 maximum iterations. After 100 runs, the optimum objective function value is determined. Under different settings of the proposed method, the outcomes with the least objective values are chosen for the convergence curve.

The Rao algorithm improves the result by considering the difference between the best and worst solutions. The new value of a variable is obtained by adding the difference between the best and worst values of a variable multiplied by a randomly generated number during the iteration. The algorithm improves the result by considering the difference between the best and worst solutions and considering the candidate solutions' random interactions. In the Rao algorithm, all the accepted function values at the end of the iteration are maintained. These values become the input to

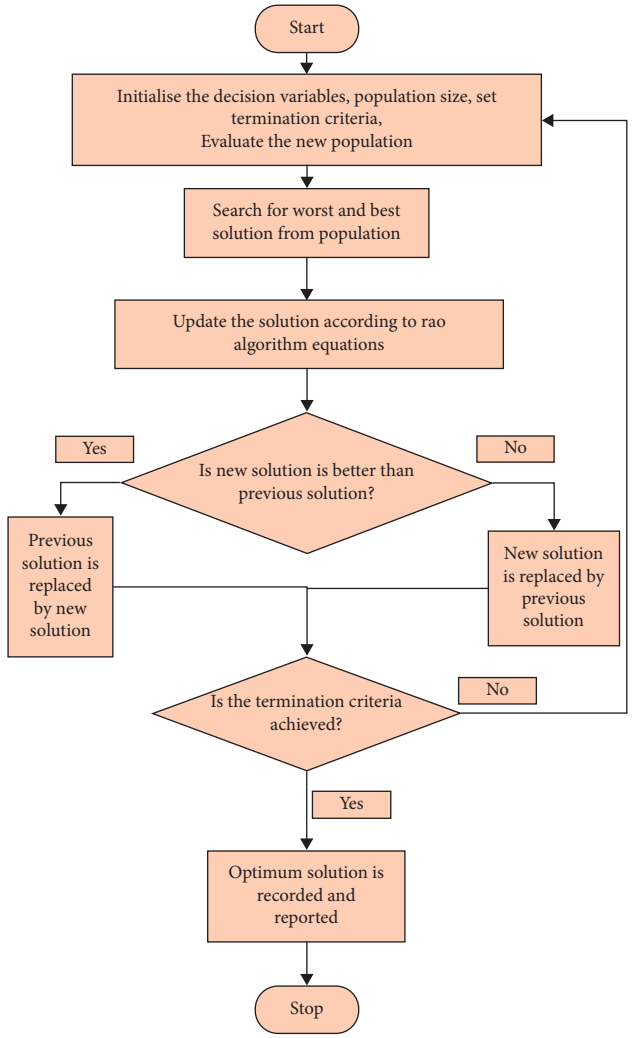

Figure 6: Flowchart of Rao algorithm.

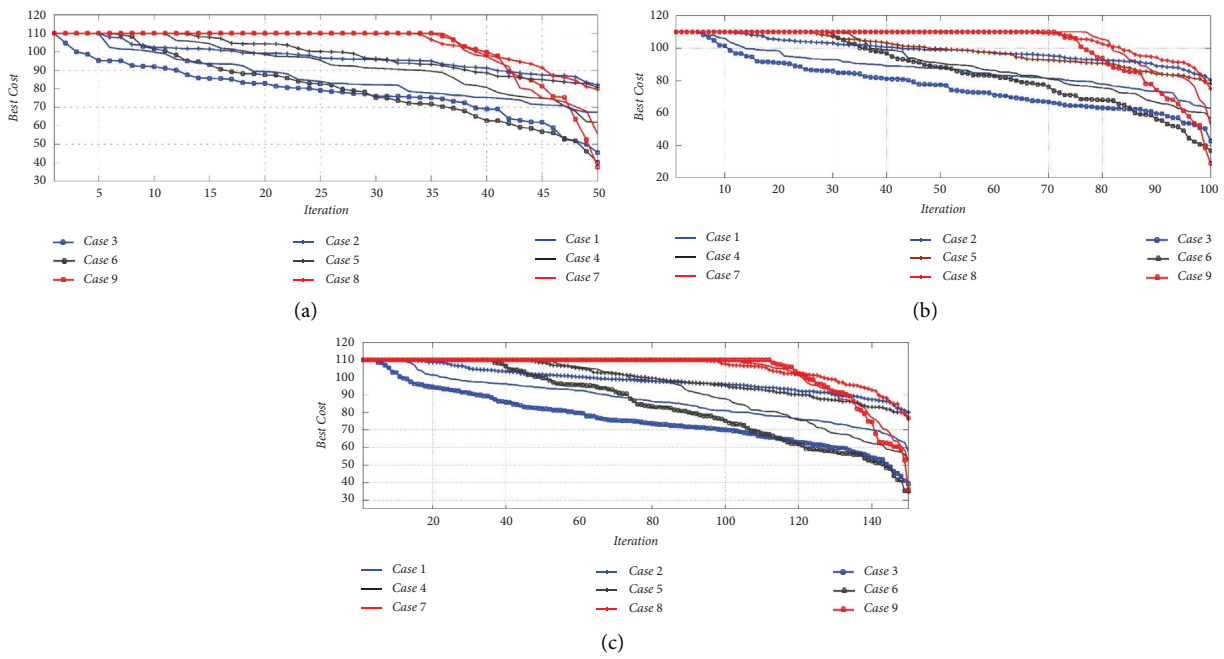

Figure 7: Convergence characteristic for constant load with (a) 50 (b) 100, and (c) 150 iterations.

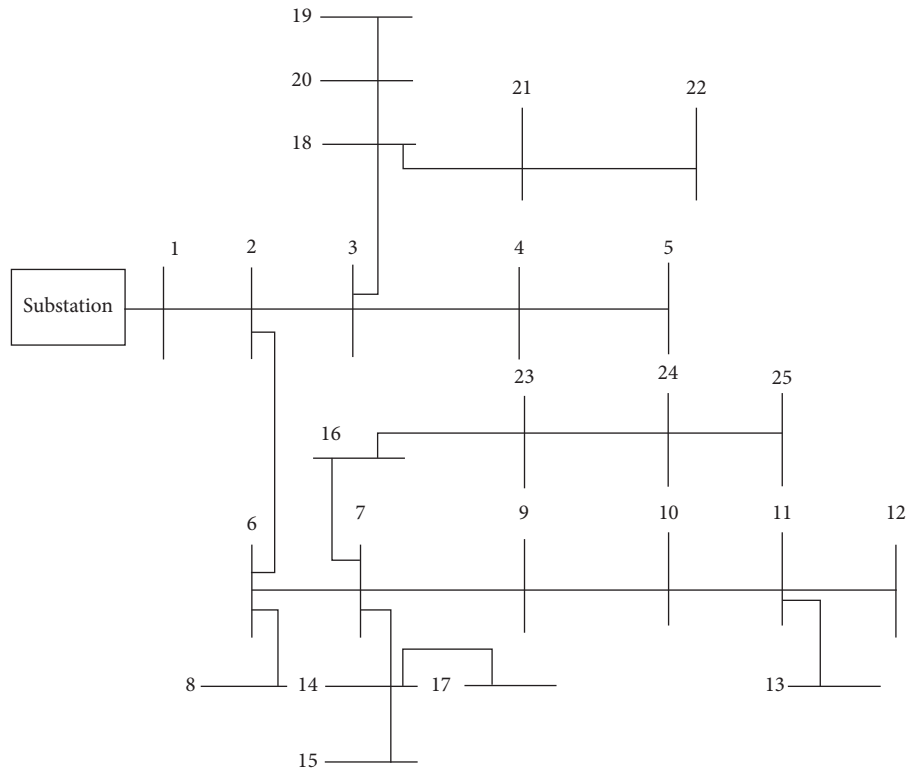

Figure 8: Single line layout of 25 bus unbalanced radial distribution system.

the next iteration. The randomly generated number $r1$ used to multiply the difference between the best and worst solutions helps in the excellent exploration of the search space. The absolute value of the variable for the candidate is considered in equation (35); furthermore, equation (37) enhances the algorithm's exploration ability. The randomly generated number $r2$ is used to multiply the difference between a variable's values corresponding to a candidate and another randomly selected candidate. This helps in the acceptable exploitation of the search space. For these reasons, the Rao algorithm has been proven to have better competitive results.

7. Simulation Results

The proposed Rao optimization algorithm is tested on a standard three-phase IEEE-25 RUDS shown in Figure 8. The base value of system voltage and power is 4.16 kV and 30 MVA respectively. The IEEE-25 bus system contains 25 buses connected with 24 branches. From [40] the line and load data of the test system is taken. The investigation into the tested system was carried out under the following conditions for finding the optimal size and location of DGDST using a formulated multiobjective function:

(i) Mixed load model demand Pre COVID-19 effect

(ii) Mixed load model demand during COVID-19 effect

For the purpose of assessing objective function, the optimum placement is performed using a single, two, or three DG, DSTATCOM, or both DG and DSTATCOM. The size of DGDST is maintained within a specific range. The lowest range is zero, and the maximum range is equal to the loading on each phase. All instances are evaluated using setting 3 of the suggested method in this load due to its superior performance in covering all the possibilities and effectively utilizing the exploration and exploitation of the optimization algorithm. The simulation results are described in the following section.

7.1. Mixed LMs. Table 3 includes the optimal allocation results phase-wise for DG and DSTATCOM for all the cases, pre-COVID-19 effect. The global minima of multiobjective functions are obtained for the values of size and location of DGDST for each case. For single DG and DSTATCOM individual allocation problems, bus location 7 was found optimal, whereas for single DG and DSTATCOM together, bus location 7 was found optimal for DG and bus location 9 was found optimal for DSTATCOM. It is revealed from the table that a particular bus is found optimal for all the phases because different bus locations for different phases introduced phase unbalancing into the unbalanced distribution system.

Table 4 summarizes the phase-wise outcome of all stages for all cases after allocation of DG and DSTATCOM, pre-COVID-19 effect. The value of APL and RPL decreased, whereas the MVV and VSI magnitude increased. The APL is 40.759 kW for phase a, 43.192 kW for phase b, and 33.583 kW for phase c in the basic scenario, which is decreased to 19.83 kW, 20.989 kW, and 16.627 kW for PhABC in Case1, respectively. Furthermore, it decreased to

Table 3: The optimal size and location of DG and DSTATCOM for mixed LM pre-COVID-19 effect.

Description		DG size in kW (bus)			DSTATCOM size in kVar (bus)		
		Phase A	Phase B	Phase C	Phase A	Phase B	Phase C
Case 1	1DG	442.54 (7)	712.78 (7)	626.93 (7)			
Case 2	1DSTATCOM				406.21 (7)	434.23 (7)	436.08 (7)
Case 3	1DGDST	951.32 (7)	1002 (7)	420.05 (7)	357.97 (9)	494.96 (9)	468.76 (9)
Case 4	2DG	585.41 (4), 294.12 (10)	314.07 (4), 367.22 (10)	148.31 (4), 438.71 (10)			
Case 5	2DSTATCOM				288.18 (4), 298.72 (7)	33.784 (4), 375.41 (7)	59.458 (4), 529.54 (7)
Case 6	2DGDST	147.32 (10), 352.01 (6)	418.46 (10), 844.63 (6)	110.94 (10), 417.31 (6)	210.81 (11), 132.92 (4)	278.77 (11), 403.02 (4)	276.77 (11), 355.52 (4)
Case 7	3DG	272.16 (10), 249.29 (15), 224.66 (21)	118.92 (10), 381.17 (15), 148.22 (21)	145.77 (10), 297.52 (15), 308.80 (21)			
Case 8	3DSTATCOM				373.37 (3), 222.18 (7), 103.96 (9)	361.28 (3), 365.72 (7), 156.11 (9)	193.66 (3), 325.26 (7), 34.482 (9)
Case 9	3DGDST	306.44 (23), 747.24 (6), 379.35 (18)	169.6 (23), 417.7 4(6), 488.53 (18)	22.794 (23), 928.6 (6), 186.3 (18)	560.7 (3), 327.22 (15), 53.584 (14)	312.61 (3), 397.16 (15), 87.238 (14)	463.32 (3), 107.85 (15), 18.179 (14)

Table 4: The phase wise result analysis for mixed LM pre COVID-19 effect.

Description	Phase A				Phase B				Phase C			
	APL (kW)	RPL (kVar)	MVV (p.u.)	VSI (p.u.)	APL (kW)	RPL (kVar)	MVV (p.u.)	VSI (p.u.)	APL (kW)	RPL (kVar)	MVV (p.u.)	VSI (p.u.)
Base case	40.759	45.442	0.93881	0.77368	43.192	41.399	0.93827	0.77122	33.583	44.872	0.94491	0.79378
Case 1	19.834	24.293	0.96179	0.85243	20.989	17.732	0.96948	0.88316	16.627	22.078	0.9678	0.87373
Case 2	33.176	36.413	0.95675	0.83467	34.674	33.179	0.95599	0.83129	26.82	35.136	0.96349	0.85821
Case 3	17.198	14.337	0.97965	0.92084	18.682	15.665	0.9781	0.91501	15.307	19.23	0.97401	0.89974
Case 4	16.908	16.513	0.96608	0.86846	18.462	17.093	0.96612	0.86852	15.406	21.281	0.96841	0.87619
Case 5	30.344	32.766	0.95777	0.83821	36.314	33.592	0.9525	0.81922	25.929	36.504	0.96988	0.88126
Case 6	11.921	15.974	0.97441	0.90129	17.642	16.759	0.99127	0.96531	14.106	13.901	0.97423	0.89752
Case 7	14.404	15.593	0.96995	0.88492	16.269	16.76	0.96876	0.87676	12.532	15.491	0.97153	0.8874
Case 8	31.555	35.72	0.96091	0.84928	31.734	31.804	0.97032	0.88242	27.718	31.101	0.96202	0.85298
Case 9	15.35	14.998	0.99751	0.9864	12.86	10.833	0.98694	0.94435	12.889	10.583	0.98279	0.9293

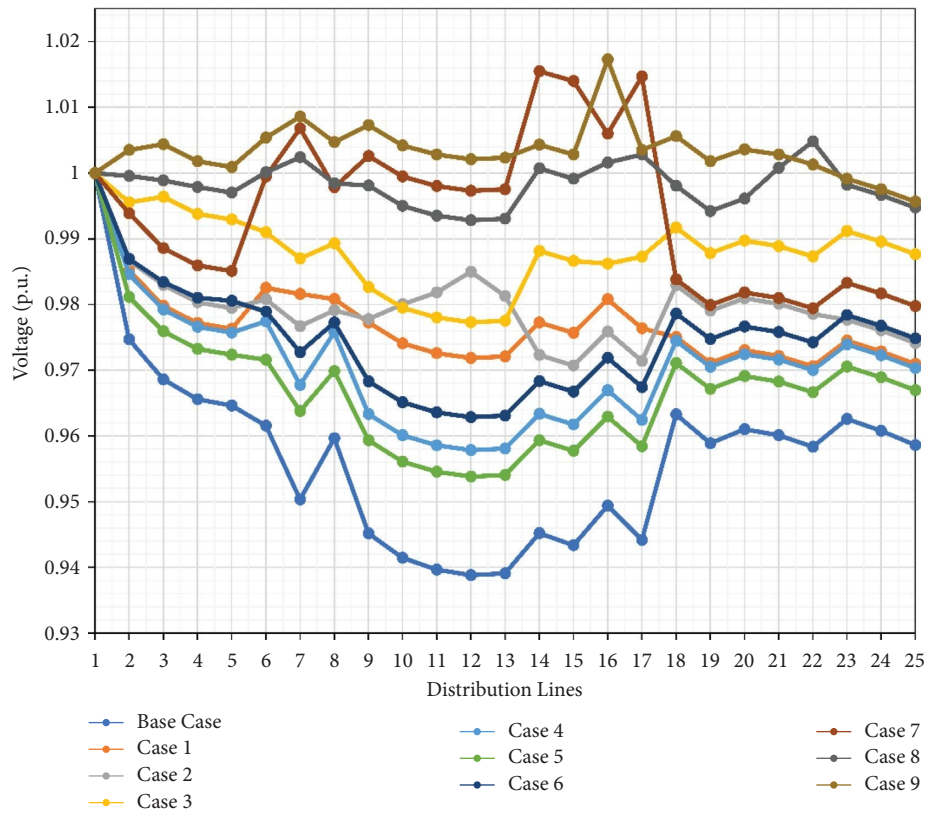

Figure 9: Comparison of voltage profile of phase *a* of all the cases for mixed LM pre-COVID-19 effect.

33.176 KW, 34.67 KW, and 26.82 KW for PhABC, respectively. It is found that with DG allocation, minimum values are obtained for APL compared to DSTATCOM allocation. Furthermore, the combined allocation of DGDST (Case 3) provided the best outcome, minimizing the APL of 17.198 KW, 18.682 KW, and 15.307 KW, respectively, to a minimum level compared to cases 1 and 2.

The RPL is also decreased for PhABC to 15.593 kVar, 16.76 kVar, and 15.491 kVar from 45.442 kVar, 41.399 kVar, and 44.872 kVar in the primary case. For PhABC, the MVV was increased from 0.93881 p.u., 0.93827 p.u., and 0.94491 p.u. to 0.96995 p.u., 0.96876 p.u., and 0.97153 p.u. In addition, the VSI was increased for PhABC from 0.77368 p.u., 0.77122 p.u., and 0.79378 p.u. to 0.88492 p.u., 0.87676 p.u., and 0.8874 p.u. Following DG, DSTATCOM is positioned ideally inside the distribution system to maximize performance. After repeated allocation of DSTATCOM, the APL for PhABC decreased to 31.555 kVar, 31.734 kVar, and 27.718 kVar, respectively. In addition, the RPL for PhABC is reduced to 35.72 kVar, 31.804 kVar, and 31.101 kVar, respectively, compared to the original base case result. In addition, PhABC optimizes the MVV to 0.96091 p.u., 0.97032 p.u., and 0.96202 p.u. from 0.84928 p.u., 0.88242 p.u., and 0.85298 p.u. are the improved VSI values for PhABC. It was concluded from the findings that although DSTATCOM installation decreases APL and RPL and increases MVV and VSI, it exhibits less improvement in objective function than DG placement, implying that concurrent deployment of DG and DSTATCOM would enhance outcomes in a more stressful situation. Therefore, it is revealed that the allocation of DGDST is a better approach compared to the individual allocation of DG and DSTATCOM.

The voltage profile is shown in Figure 9 for all cases considered. The voltage profile enhanced significantly from the base case to sequential cases. It is clear from the voltage profile that the voltage of all the phases is within tolerance limits. However, the 3DGDST allocation (Case 9) provides the best voltage profile compared to other cases.

From the above-given results, it is clear that the obtained optimal values provided an excellent outcome by reducing the APL and RPL values as well as maximizing the MVV and VSI values for the unbalanced distribution system for the pre-COVID-19 scenario. The same approach to the allocation of DG and DSATCOM individually and together will be applied to mixed load model demand during COVID-19 in the next section.

7.2. Mixed LMs during COVID-19 Effect. In COVID-19, demand is influenced by the fluctuations in load demand according to different classes of consumers with positive and negative load growth described in section 2 (COVID-19 effect).

Table 5 summarizes the optimal results for DG and DSTATCOM allocation. The location and size obtained for all the cases were different compared to the pre-COVID-19 LM due to unpredicted load demand oscillation.

Table 5: The optimal size and location of DG and DSTATCOM for mixed LM during COVID-19 effect.

Description		DG size in kW (bus)			DSTATCOM size in kVar (bus)		
		Phase A	Phase B	Phase C	Phase A	Phase B	Phase C
Case 1	1DG	517.24 (7)	478.43 (7)	470.4 (7)			
Case 2	1DSTATCOM				360.34 (6)	469.48 (6)	238.8 (6)
Case 3	1DGDST	837.58 (14)	540.33 (14)	779.58 (14)	339.2 (7)	522.08 (7)	328.6 (7)
Case 4	2DG	290.79 (12), 304.09 (18)	489.24 (12), 429.28 (18)	215.04 (12), 641.61 (18)			
Case 5	2DSTATCOM				86.87 (3), 182.19 (7)	416 (3), 332.07 (7)	356.84 (3), 259.91 (7)
Case 6	2DGDST	212.33 (23), 511.95 (7)	489.18 (23), 510.93 (7)	413.49 (23), 178.67 (7)	320.41 (22), 243.72 (17)	292.77 (22), 356.3 (17)	176.99 (22), 378.48 (17)
Case 7	3DG	903.34 (3), 95.311 (6), 332.12 (14)	668.5 (3), 178.29 (6), 124.3 (14)	423.31 (3), 418.34 (6), 99.955 (14)			
Case 8	3DSTATCOM				40.58 (5), 175.76 (3), 297.09 (7)	72.051 (5), 317.22 (3), 323.4 (7)	103.53 (5), 20.023 (3), 465.38 (7)
Case 9	3DGDST	189.49 (30), 608.37 (16), 55.772 (18)	902.47 (3), 384.43 (16), 154.98 (18)	624.72 (3), 503.24 (16), 298.57 (18)	396.83 (18), 72.273 (8), 243.58 (9)	121.5 (18), 243.08 (8), 221.9 (9)	278.99 (18), 202.55 (8), 128.74 (9)

Table 6: The phase wise result analysis for mixed LM during COVID-19 effect.

Description	Phase A				Phase B				Phase C			
	APL (kW)	RPL (kVar)	MVV (p.u.)	VSI (p.u.)	APL (kW)	RPL (kVar)	MVV (p.u.)	VSI (p.u.)	APL (kW)	RPL (kVar)	MVV (p.u.)	VSI (p.u.)
Base case	40.987	45.683	0.93850	0.77263	43.44	41.641	0.93798	0.77025	33.753	45.118	0.94461	0.79277
Case 1	14.606	16.166	0.97059	0.88728	16.313	15.805	0.96906	0.87835	13.004	18.045	0.97043	0.88374
Case 2	29.084	33.088	0.95784	0.8389	29.404	27.957	0.96085	0.84891	26.57	31.855	0.95697	0.83561
Case 3	17.273	15.342	0.97944	0.92007	14.46	12.987	0.98045	0.92389	13.896	13.246	0.98161	0.92821
Case 4	12.086	13.793	0.9707	0.88562	17.144	13.093	0.98065	0.92237	14.092	16.121	0.96692	0.87124
Case 5	30.769	33.437	0.95381	0.82485	28.362	30.986	0.96819	0.87521	22.094	27.407	0.96904	0.87865
Case 6	11.564	10.138	0.99282	0.96852	14.005	9.9302	0.99372	0.97126	16.507	14.36	0.97776	0.91065
Case 7	13.802	14.459	0.97729	0.90932	12.613	12.392	0.96503	0.86389	9.7675	11.554	0.9717	0.88844
Case 8	28.383	30.861	0.96285	0.8566	28.805	28.991	0.96555	0.86569	24.542	30.253	0.97357	0.89525
Case 9	13.451	12.258	0.99566	0.98256	15.559	13.849	1	1	9.4786	11.708	0.9957	0.9796

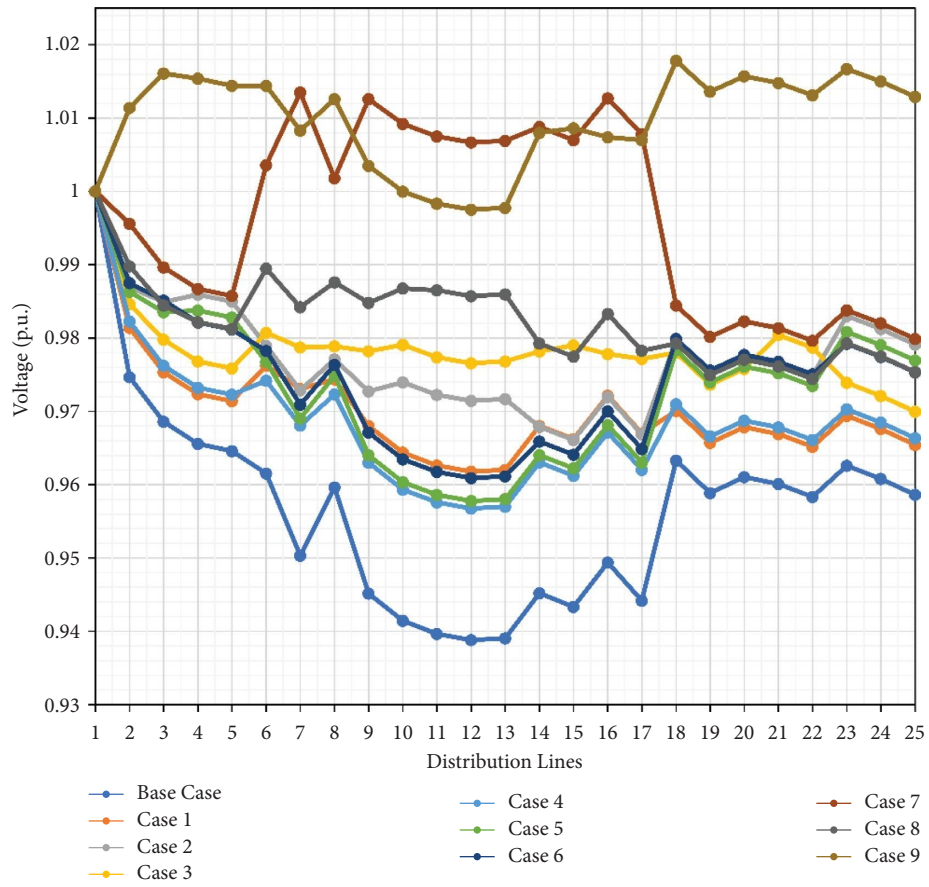

Figure 10: Comparison of voltage profile of phase *a* of all the cases for mixed LM during COVID-19 effect.

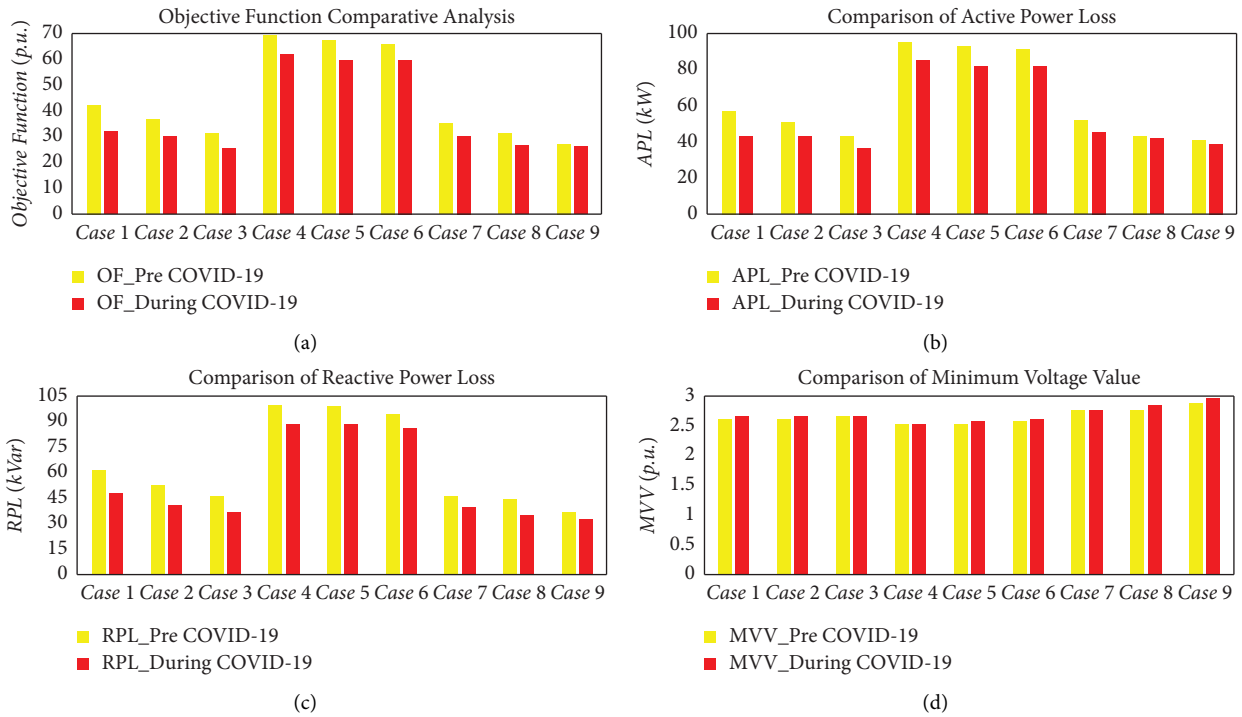

Figure 11: Continued.

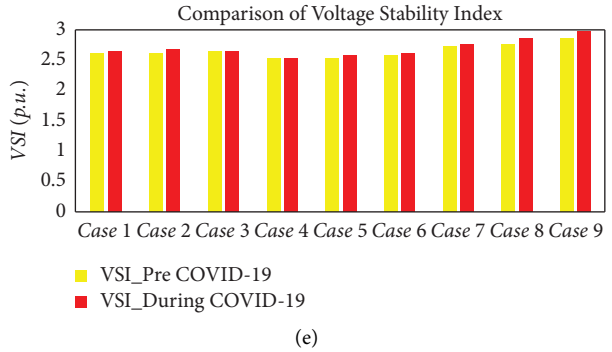

(e)

Figure 11: Comparison graph for all the cases for mixed LM pre- and during COVID-19 effect of (a) OF, (b) APL, (c) RPL, (d) MVV, and (e) VSI.

Table 6 summarizes the results followed by the optimal allocation of DG and DSTATCOM for various formed cases. A similar trend is observed in COVID-19 load demand after optimal allocation of DG and DSTATCOM from Cases 1 to 9. The best result was obtained for Case 9, like the previous pre-COVID-19 scenario.

In the basic scenario, the APLs for phases a, *b*, and *c* are 40.987 kW, 43.44 kW, and 33.753 kW, respectively, which are lessened to 13.802 kW, 15.559 kW, and 9.4786 kW for PhABC following multiple DGDST allocations in Case 9. In addition, RPL is decreased to 12.258 kVar, 13.849 kVar, and 11.708 kVar for PhABC in Case 9, down from 45.683 kVar, 41.641 kVar, and 45.118 kVar in the base case.

In Case 9 For PhABC, MVV increased from 0.9385 p.u., 0.93798 p.u., and 0.94461 p.u. to 0.99566 p.u., 1 p.u., and 0.9957 p.u. respectively. Furthermore, the VSI for PhABC increased from 0.77263 p.u., 0.77025 p.u., and 0.79277 p.u. to 0.98256 p.u., 1 p.u., and 0.9796 p.u., respectively.

It is evident again from the findings for Cases 1 to Case 9 that although DSTATCOM installation reduces APL and RPL and increases MVV and VSI, it exhibits less improvement in objective function than DG placement, implying that concurrent deployment of DG and DSTATCOM would enhance outcomes in a more vital COVID-19 situation.

The voltage profile is shown in Figure 10 for all the considered cases. As can be seen from the graph, under the mixed load model, demand improvement is enhanced from Case 1 to Case 9. Again, the combination of 3DGDST produced the best voltage profile compared to other cases.

7.2.1. Comparative Analysis of Pre and during COVID-19 Situations. From Figures 7, 9, and 10, it is clear that the optimal allocation of DG and DSTATCOM by the Rao algorithm improves the performance of the distribution network. However, the 3DGDST (Case 9) found an optimal solution because of maximum improvement and the equivalent resolution in both pre- and during the COVID-19 situation, making the distribution grid more resilient to emergency situations caused by highly unpredictable nonuniform load demand scenarios. Figure 11 presented the comparative graphs for all the cases of mixed LM pre- and during COVID-19 effect.

8. Conclusion

In the presented work, the optimal allocation of DGDST is done using the Rao optimization algorithm with mixed load models. The effect of COVID-19 was analysed by taking into account the variation in load demand during the lockdown period. The optimal value of single, two, and three DG, DSTACOM, and combined DGDST are evaluated for minimization of active and reactive power loss, and maximization of MVV and VSI considering a multiobjective function. The OF is minimized when DG is placed. The addition of DSTATCOM also gives better results, but when simultaneously DGDST is sited at optimal size, the OF is minimized by enhancing voltage profile, MVV, VSI, and reducing APL and RPL. This makes the distribution system more reliable and resilient to any critical load demand scenario. The size and location of DGDST during COVID-19 confirms the validity of the proposed approach using Rao optimization. The integration of DGDST improved the performance of the unbalanced radial distribution system for any fluctuation in the load demand scenario. Finally, all results show that maximum improvement in DS can be achieved when 3DGDST is allocated simultaneously compared to other cases.

The allocation of DG varies according to the load type and demand, so this study will help the DS operator to select a DGDST combination of the desired rating at the proper location for mixed load demand through the proposed innovative approach. The present work can be extended by using time interdependence modelling in combination with various voltage-dependent static and dynamic load models headed for optimal allocation of renewable sources-based DG. COVID-19 has disturbed the DS financially and technically, suggesting researchers for optimal planning of the EDS with the negative rise in load demand that industrial and commercial users have encountered for the first time in the history of the electricity era.

Data Availability

The data used to support the study are included in the paper. For the data related query, kindly contact to Baseem Khan basseemk@hu.edu.et.

Conflicts of Interest

The authors declare that they have no conflicts of interest.

References

[1] C. Bertram, G. Luderer, F. Creutzig et al., "COVID-19-induced low power demand and market forces starkly reduce CO2 emissions," *Nature Climate Change*, vol. 11, no. 3, pp. 193–196, 2021.

[2] S. Bhattacharya, R. Banerjee, A. Liebman, and R. Dargaville, "Analysing the impact of lockdown due to the COVID-19 pandemic on the Indian electricity sector," *International Journal of Electrical Power & Energy Systems*, vol. 141, Article ID 108097, 2022.

[3] S. Lakshminarayana, J. Ospina, and C. Konstantinou, "Load-altering attacks against power grids under COVID-19 low-inertia conditions," *IEEE Open Access Journal of Power and Energy*, vol. 9, pp. 226–240, 2022.

[4] A. Roosta, H. R. Eskandari, and M. H. Khooban, "Optimization of radial unbalanced distribution networks in the presence of distribution generation units by network reconfiguration using harmony search algorithm," *Neural Computing & Applications*, vol. 31, no. 11, pp. 7095–7109, 2019.

[5] A. Selim, S. Kamel, A. S. Alghamdi, and F. Jurado, "Optimal placement of DGs in distribution system using an improved harris hawks optimizer based on single- and multi-objective approaches," *IEEE Access*, vol. 8, pp. 52815–52829, 2020.

[6] S. R. Biswal and G. Shankar, "Simultaneous optimal allocation and sizing of DGs and capacitors in radial distribution systems using SPEA2 considering load uncertainty," *IET Generation, Transmission & Distribution*, vol. 14, no. 3, pp. 494–505, 2020.

[7] A. El-Zonkoly, "Optimal placement of multi-distributed generation units including different load models using particle swarm optimization," *Swarm and Evolutionary Computation*, vol. 1, pp. 50–59, 2011.

[8] E. El-saadany, "The effect of DG on power quality in a deregulated environment," *Proc. IEEE Power Eng. Soc. Gen. Meet.*vol. 3, pp. 2969–2976, 1999.

[9] S. Rezaeian-Marjani, S. Galvani, V. Talavat, and M. Farhadi-Kangarlu, "Optimal allocation of D-STATCOM in distribution networks including correlated renewable energy sources," *International Journal of Electrical Power & Energy Systems*, vol. 122, Article ID 106178, 2020.

[10] A. R. Gupta and A. Kumar, "Deployment of distributed generation with D-FACTS in distribution system: a comprehensive analytical review," *IETE Journal of Research*, vol. 68, no. 2, pp. 1195–1212, 2019.

[11] A. A. Eajal, M. E. El-Hawary, and L. Fellow, "Optimal capacitor placement and sizing in unbalanced distribution systems with harmonics consideration using particle swarm optimization," *IEEE Transactions on Power Delivery*, vol. 25, no. 3, pp. 1734–1741, 2010.

[12] G. Darling, J. C. Wang, T. Jianzhong, and G. Darling, "Optimal capacitor placement, replacement and control in large-scale unbalanced distribution systems: system solution algorithms and numerical studies," *IEEE Transactions on Power Systems*, vol. 10, no. 1, pp. 363–369, 1995.

[13] S. Paul, *Optimal size and location of distributed generation and KVAR support in unbalanced 3- <1> distribution system using PSO*, IEEE, Piscataway, NJ, USA, 2012.

[14] M. Gomez-Gonzalez, F. Ruiz-Rodriguez, and F. Jurado, "Probabilistic optimal allocation of biomass fueled gas engine in unbalanced radial systems with metaheuristic techniques," *Electric Power Systems Research*, vol. 108, pp. 35–42, 2014.

[15] P. Samal, S. Ganguly, and S. Mohanty, "Planning of unbalanced radial distribution systems using differential evolution algorithm," *Energy Syst*, vol. 8, no. 2, pp. 389–410, 2016.

[16] R. A. Almasri, R. Akram, A. F. Almarshoud, H. M. Omar, M. S. Alshitawi, and K. Khodary Esmaeil, "Evaluation of the total exergy and energy consumptions in residential sector in Qassim Region, Saudi Arabia," *Alexandria Engineering Journal*, vol. 62, pp. 455–473, 2023.

[17] R. Madurai Elavarasan, G. Shafiullah, K. Raju et al., "COVID-19: impact analysis and recommendations for power sector operation," *Applied Energy*, vol. 279, Article ID 115739, 2020.

[18] H. Zhong, Z. Tan, Y. He, L. Xie, and C. Kang, "Implications of COVID-19 for the electricity industry: a comprehensive review," *CSEE Journal of Power and Energy Systems*, vol. 6, no. 3, pp. 489–495, 2020.

[19] S. Dawn, S. Shree Das, S. Gope, B. Dey, and F. P. García Márquez, "Global power and energy scenario during COVID-19 pandemic : lessons from lockdown," *International Journal of Electrical Power & Energy Systems*, vol. 137, Article ID 107757, 2022.

[20] V. V. S. N. Murty and A. Kumar, "Impact of D-STATCOM in distribution systems with load growth on stability margin enhancement and energy savings using PSO and GAMS," *International Transactions on Electrical Energy Systems*, vol. 28, no. 11, pp. e2624–24, 2018.

[21] V. Andreoni, "A multiscale integrated analysis of the COVID-19 restrictions : the energy metabolism of UK and the related socio-economic changes," *Journal of Cleaner Production*, vol. 363, Article ID 132616, 2022.

[22] I. Pes, "Sharing knowledge on electrical energy industry's first response to COVID-19," 2020, https://resourcecenter.ieee-pes.org/publications/white-papers/PES_TP_COVID19_050120.html.

[23] Z. Li, H. Ye, N. Liao, R. Wang, Y. Qiu, and Y. Wang, "Impact of COVID-19 on electricity energy consumption : a quantitative analysis on electricity," *International Journal of Electrical Power & Energy Systems*, vol. 140, Article ID 108084, 2022.

[24] A. Rezaee Jordehi, "Allocation of distributed generation units in electric power systems: a review," *Renewable and Sustainable Energy Reviews*, vol. 56, pp. 893–905, 2016.

[25] R. Sirjani and A. Rezaee Jordehi, "Optimal placement and sizing of distribution static compensator (D-STATCOM) in electric distribution networks: a review," *Renewable and Sustainable Energy Reviews*, vol. 77, pp. 688–694, 2017.

[26] R. V. Rao, "Rao algorithms: three metaphor-less simple algorithms for solving optimization problems," *International Journal of Industrial Engineering Computations*, vol. 11, no. 1, pp. 107–130, 2020.

[27] R. V. Rao and H. S. Keesari, "Rao algorithms for multi - objective optimization of selected thermodynamic cycles," *Engineering with Computers*, vol. 37, no. 4, pp. 3409–3437, 2020.

[28] A. K. Bohre, G. Agnihotri, and M. Dubey, "Optimal sizing and sitting of DG with load models using soft computing

techniques in practical distribution system," *IET Generation, Transmission & Distribution*, vol. 10, no. 11, pp. 2606–2621, 2016.

[29] K. R. Devabalaji and K. Ravi, "Optimal size and siting of multiple DG and DSTATCOM in radial distribution system using Bacterial Foraging Optimization Algorithm," *Ain Shams Engineering Journal*, vol. 7, no. 3, pp. 959–971, 2016.

[30] N. Acharya, P. Mahat, and N. Mithulananthan, "An analytical approach for DG allocation in primary distribution network," *International Journal of Electrical Power & Energy Systems*, vol. 28, no. 10, pp. 669–678, 2006.

[31] S. Khushalani, J. M. Solanki, and N. N. Schulz, "Development of three-phase unbalanced power flow using PV and PQ models for distributed generation and study of the impact of DG models," *IEEE Transactions on Power Systems*, vol. 22, no. 3, pp. 1019–1025, 2007.

[32] E. Conversion, "Optimal placement of DSTATCOM , DG and their performance analysis in deregulated power system surajit sannigrahi ∗ sriparna roy ghatak debarghya basu and parimal acharjee," *International Journal of Power and Energy Conversion*, vol. 10, no. 1, pp. 105–128, 2019.

[33] O. P. Mahela and A. G. Shaik, "A review of distribution static compensator," *Renewable and Sustainable Energy Reviews*, vol. 50, pp. 531–546, 2015.

[34] S. Skarvelis-kazakos, M. Van Harte, M. Panteli et al., "Resilience of electric utilities during the COVID-19 pandemic in the framework of the CIGRE definition of Power System Resilience," *International Journal of Electrical Power & Energy Systems*, vol. 136, Article ID 107703, 2022.

[35] Central Electricity Authority (Cea), *Growth of Electricity Sector in india from 1947-2019*, Central Electricity Authority, New Delhi, India, 2019.

[36] T. Gözel, M. H. Hocaoglu, U. Eminoglu, and A. Balikci, "Optimal placement and sizing of distributed generation on radial feeder with different static load models," in *Proceedings of the 2005 International Conference on Future Power Systems*, pp. 1–6, Amsterdam, Netherlands, November 2005.

[37] D. Singh, D. Singh, and K. S. Verma, "Multiobjective optimization for DG planning with load models," *IEEE Transactions on Power Systems*, vol. 24, no. 1, pp. 427–436, 2009.

[38] S. M. Mahfuz Alam and M. H. Ali, "Analysis of COVID-19 effect on residential loads and distribution transformers," *International Journal of Electrical Power & Energy Systems*, vol. 129, Article ID 106832, 2021.

[39] J. Teng and C. Chang, "A novel and fast three-phase load flow for unbalanced radial distribution systems," *IEEE Transactions on Power Systems*, vol. 17, no. 4, pp. 1238–1244, 2002.

[40] T. Ramana, V. Ganesh, and S. Sivanagaraju, "Distributed generator placement and sizing in unbalanced radial distribution system," *Cogeneration and Distributed Generation Journal*, vol. 25, no. 1, pp. 52–71, 2010.